Original Article

Enhanced Adsorption of Methylene Blue Dye from Water by Alkali-Treated Activated Carbon

Segun Michael Abegunde* | **Kayode Solomon Idowu**

Department of Science Technology, Federal Polytechnic, Ado-Ekiti, Ekiti State, Nigeria

Use yor device to scan and read the article online

Citation S. M. Abegunde, K. S. Idowu. **Enhanced Adsorption of Methylene Blue Dye from Water by Alkali-Treated Activated Carbon.** *Eurasian J. Sci. Technol.*, **2023**,*3*(3), 109-124.

https://doi.org/10.48309/ejst.2023.379937.1078

Article info:
Received: 2023-01-10
Accepted: 2023-02-27
Available Online: 2023-03-03
ID: EJST-2301-1078
Checked for Plagiarism: Yes
Checked Language: Yes

Keywords:

Methylene blue, *Raphia taedigera*, Alkali-modification, Dye pollution, Activated, Carbon, Wastewater.

ABSTRACT

In this work, activated carbon (AC) was prepared from *Raphia taedigera* seed and modified with sodium hydroxide (0.1 M) solution. The activated carbon (RTB) and the untreated *Raphia taedigera* raw (RTR) seed powder were characterised and engaged to remove Methylene blue (MB) dye from aqueous solution. Both materials were characterized by Fourier-transform infrared spectroscopy (FTIR) and Scanning electron microscopy (SEM). FTIR revealed the presence of functional groups such as hydroxyl, carboxylic, alkenes, aldehydes, and ketonic groups. SEM image showed the surface morphology of the material is characterized by aggregated structure with pores. The performances evaluation of the materials gave the highest percentage of MB dye removal of 84.21 and 97.00% were observed for RTR and RTB, respectively, at pH 5. The adsorption modelling showed that the MB dye adsorption onto both adsorbents could best be represented by Langmuir isotherm and followed the pseudo-second-order kinetic model. The thermodynamic studies predicted exothermic, feasible, spontaneous, and physisorption nature of MB dye adsorption onto the RTR and RTB within the temperature range for this study.

Introduction

Textile industry is known as one of the biggest industries since ancient times for its industrial, economical, and environmental impacts. The industry consumes about two-thirds of over 700,000 metric tonnes of approximately 10000 commercially available dyestuff produced annually [1]. However, nearly 15% of the commonly used synthetic dyes consumed yearly are lost to industrial effluents at different stages of the dying process [2]. Due to their excellent solubility in water, synthetic dyes force their paths through to the surrounding water bodies. The presence of some dyes in water, even as low as 1 ppm or less is highly noticeable and undesirable [3]. The complexity of dyes' aromatic molecular structures enhances their stability and slows down biodegradability. Bioaccumulation of dye molecules in water may cause a potential

***Corresponding Author:Segun Michael Abegunde** (abegundes@gmail.com)

hazard to the aquatic environment, and may affect man through the food chain. Dye presence in water bodies also blocks light penetration, and thus, affect photosynthesis significantly [4].

Methylene blue (MB) dye is a cationic dye usually used for materials colouring. Indiscriminate discharge of MB dye wastes into the surroundings can lead to cyanosis, nausea, diarrhoea, gastrointestinal tract, skin irritation, and convulsions, if consumed [5]. Dyes and their derivatives can be toxic, mutagenic, and carcinogenic [6]. Therefore, wastewater decontamination becomes environmentally essential.

Prior to this time, some commonly used conventional methods for water and wastewater treatment include the Fenton process, sonochemical degradation, reverse osmosis, chemical coagulation, flocculation, chemical precipitation, oxidation, ozonation, chemical precipitation, ion exchange, adsorption, and modified processes [7,8]. However, adsorption has proved to the best method for dye removal from wastewaters in recent times [1,9,10]. Adsorption is a prominent and highly effective technique for dye removal from wastewaters. In recent years, the adsorption has been extensively engaged to retrieve organic and inorganic pollutants from wastewaters. The technique has advantages over other conventional wastewater treatment methods because of its low-cost, design simplicity, ease of operation, and high efficiency [11].

Activated carbons (ACs) are known for their large surface area, high micro-porosity, homogenous structure, radiation stability, and strong adsorption capacity, which enable them to fare well in water treatment processes [12]. These essential adsorption-bond features can be attained through a selective surface treatment of the material by physical or chemical surface treatment or combination of both. Chemical surface modification transforms materials into valuable products with high adsorptive capacities differ from precursor. The process impacts onto the material new surface properties not find in the precursor [13,14]. Nowadays, the focus is being shifted to agro-wastes as precursors to prepare activated carbons to serve as inexpensive and effective alternatives to existing high-cost commercial activated carbons [15].

Raphia taedigera, a cespitous and monocarpic plant species, grows in Brazil, Cameroon, Costa Rica, Nigeria, and Panama [16,17]. *R. taedigera* produces a brown chicken egg-sized seed. *Raphia taedigera* seed activated carbon impregnated with hydrochloric acid had been reported for its efficiency for the removal of MB dye molecules from aqueous solution [18]. Therefore, the present work aimed to evaluate the performance of alkali-treated activated carbon prepared from *R. taedigera* seed for the removal of methylene blue dye from aqueous solution which until now has not be reported.

Experimental

Raphia Taedigera Activated Carbon

Seeds of *Raphia taedigera* were collected in Ise-Ekiti, Nigeria, and separated from dirt, washed, sun-dried for 30 days, and crushed. The activated carbon was prepared using a method reported by Olasehinde and Abegunde [15]. 50 g of crushed seed was carbonised in a furnace at 350 ^{o}C for 2 hrs. After the period of carbonisation, the new material was allowed to stand and cool to ambient temperature, washed in distilled water until the pH 7 and dried in an oven at 105 ^{o}C to obtain a constant weight. Alkali surface activation was done by soaking 20 g of the carbonised material in 100 mL 0.1 M NaOH solution in a well cleaned 500 mL beaker; the mixture was left to stand for 24 hours with thorough stirring. The excess sodium hydroxide solution used as activating agent was washed off the impregnated material to neural with distilled water and dried at 105 °C in an oven to constant weight. The treated AC was sieved with 100-mm sized mesh and the fine powder obtained was labelled RTB, while the raw *Raphia taedigera* seed named RTR. The two materials were stored separately in airtight plastic containers for further use.

Materials Characterization

FT-IR analysis was done on RTB and RTR using Agilent Cary 630 FTIR (made in US) instrument with 4000-650 cm^{-1} scanning range to determine the functional groups in the materials. Phenom Pro X SEM (Made in the Netherlands) examined the surface morphologies of the materials at HV value of 15 kV.

Preparation of Stock Solution

0.1 g MB dye was dissolved with distilled water in 1000 mL volumetric flask and made up to the mark. The content of the flask was labelled 100 mg/L MB and used as stock solution. Subsequent concentrations were prepared from the stock.

Batch Adsorption Studies

0.10 g of each adsorbent was agitated with 50 mL of MB dye stock in 250 mL conical flask. The initial pH of the solutions was adjusted to 7, using 0.1 M HCl or 0.1 M NaOH solution. The mixture was shaken at 120-rpm on shaker for 60 minutes to obtain equilibrium time. The solution was filtered and the filtrate's dye concentration was determined using UV-Vis spectrometer. The quantities of dye adsorbed (q_e) and the percentage dye uptake were determined using Equations (1) and (2), respectively. The effects of contact time, temperature, solution pH, adsorbent dosage, and adsorbate concentration on the adsorption technique were also evaluated.

$$q_e = \frac{(C_o - C_e)V}{W} \quad (1)$$

$$\%E = \frac{(C_o - C_e)}{C_o} \times 100 \quad (2)$$

Where,

C_o = initial MB dye concentration in mg/L, q_e = quantity of MB dye adsorbed per unit mass of adsorbent in mg/g, C_e = MB dye concentration at equilibrium in mg/L, W = mass of the adsorbent in g, and V = volume of MB dye solution in mL.

Adsorption Isotherm

Adsorption isotherm provides information about the adsorbent- pollutant interaction [19]. It also helps to determine the adsorbents properties such as pore size, pore volume, or energy distribution, and specific surface. Langmuir and Freundlich isotherm models were used for modelling the data from the present work.

Langmuir Isotherm

The Langmuir isotherm adsorption model is valid for single-layer adsorption. It assumes the maximum adsorption corresponds to a saturated monolayer of solute molecules on the adsorbent surface. Furthermore, it reveals the constant nature of the energy of adsorption, with no transmigration of adsorbate in the plane of the surface [20].

The Langmuir isotherm model expression is:

$$q_e = \frac{q_{max} b C_e}{1 + K_L C_e} \quad (3)$$

The linearised form of Equation 3 is:

$$\frac{C_e}{q_e} = \frac{1}{K_L q_m} + \frac{C_e}{q_m} \quad (4)$$

Where,

q_e and q_{max} = the equilibrium and the maximum amount of the dye per unit mass of adsorbent, respectively, C_e = the residual pollutant concentration at equilibrium (mg/L), and K_L = constant related to the affinity of the binding sites.

The isotherm shape in terms of separation factor (R_L) is expressed as:

$$R_L = \frac{1}{1 + KLCo} \quad (5)$$

K_L(L/mg) = Langmuir constant

C_o = the initial MB concentration in mg/L.

Freundlich Isotherm

Freundlich isotherm predicts that adsorption takes place on heterogeneous surfaces with an uneven distribution of sorption heat through a multilayer adsorption mechanism [21]. The Freundlich isotherm can be expressed as:

$$q_e = K_f\, C_e^{1/n} \quad (6)$$

The logarithmic form becomes:

$$\log q_e = \log K_f + \frac{1}{n}\log C_e \quad (7)$$

Where,

q_e = equilibrium amount adsorbed in mg/g and C_e = the pollutant concentration at (mg/L), n = Freundlich constants.

Adsorption Kinetic

Adsorption kinetic is significant for experimental applications, the process design, and operation control. The knowledge of adsorption kinetics in wastewater treatment is crucial as it gives valuable understanding of the mechanism of an adsorption process [22]. The pseudo- first- and second-orders of kinetic models were used to model the data obtained for the present work.

Pseudo-first-order Kinetic Model

Pseudo-first-order kinetic model predicts that the overall adsorption rate is directly proportional to the driving force [6]. Therefore, the pseudo-first-order kinetic model in linear form can be expressed as Equation (8).

$$\log(q_{eq} - q_t) = log\ q_{eq} - \frac{k_1 t}{2.303} \quad (8)$$

Where,

q_{eq} = amount of dye adsorbed at equilibrium (mg/g), q_t = amount of dye adsorbed at time, t (mg/g), and k_1 = equilibrium rate constant (min^{-1}).

Pseudo-second-order Kinetic Model

The pseudo-second-order reaction kinetics model is based on the absorption equilibrium capacity. The linear form is expressed as Equation (9):

$$\frac{t}{q_t} = \frac{1}{k_2 q_e^2} + \frac{1}{q_e}\ \ t \quad (9)$$

Where,

q_t = amount of dye adsorbed at time t (mg/g) and k_2 = the equilibrium rate constant for the pseudo-second-order adsorption (g/mg/min).

Thermodynamic Studies

The thermodynamic parameters values such as enthalpy change (ΔH^0), entropy (ΔS^0), and free energy (ΔG^0) provides valuable insights into temperature effect on the adsorption [22]. The thermodynamic data can be derived using Equation (10):

$$K_c = \frac{Cs}{Ce} \quad (10)$$

Where,

C_s = metal ions concentration on the ACs at equilibrium in mg/g, C_e = equilibrium concentration of dye in a solution in mg/L, and K_c = thermodynamic equilibrium constant.

The Gibbs free energy, ΔG^0(kJ/mol) for the dye adsorption onto the adsorbents can be obtained using Equation (11):

$$\Delta G^0 = -RT ln\ K_c \quad (11)$$

Entropy and enthalpy are obtained from Van't Hoff's Equation [8]:

$$\Delta G^0 = \Delta H^0 - T\Delta S^0 \quad (12)$$

$$\ln Kc = \frac{\Delta S^0}{R} - \frac{\Delta H^0}{RT} \quad (13)$$

T = absolute temperature (K), R = universal gas constant (8.314 J/mol/k), ΔH^0 =change in enthalpy, and ΔS^0 = degree of disorderliness of a reaction.

Results and Discussion

FTIR Analysis

Fourier Transform Infra-Red spectroscopy analysis was carried out on the seed (RTR) powder and the chemically modified activated carbon (RTB) to identify the different functional groups in the adsorbents. The FTIR spectra of RTR and RTB in Figures 1 and 2, respectively, revealed the complex nature of the adsorbents surfaces because of the presence of a numerous number of peaks corresponding to some essential adsorption-bond functional groups. The functional groups at band peaks of about 3650, 2300, 2100, 1500, and 1300 cm^{-1} corresponding to hydroxyl group, carboxylic group, ketonic group, alkenes, and ester group, respectively, were observed which are capable

of promoting the MB dye molecule adsorption from aqueous solution. However, additional bands at about 3700-3500, 1600-1400, 1820-1670, 1354, and 2374 cm^{-1} corresponding to hydroxyl group, alkene, carbonyl group, carboxylic group, and nitrile, respectively, were presented in RTB which can be due to the pyrolysis and chemical activation done on the material. The new development could enhance the AC adsorption capacity.

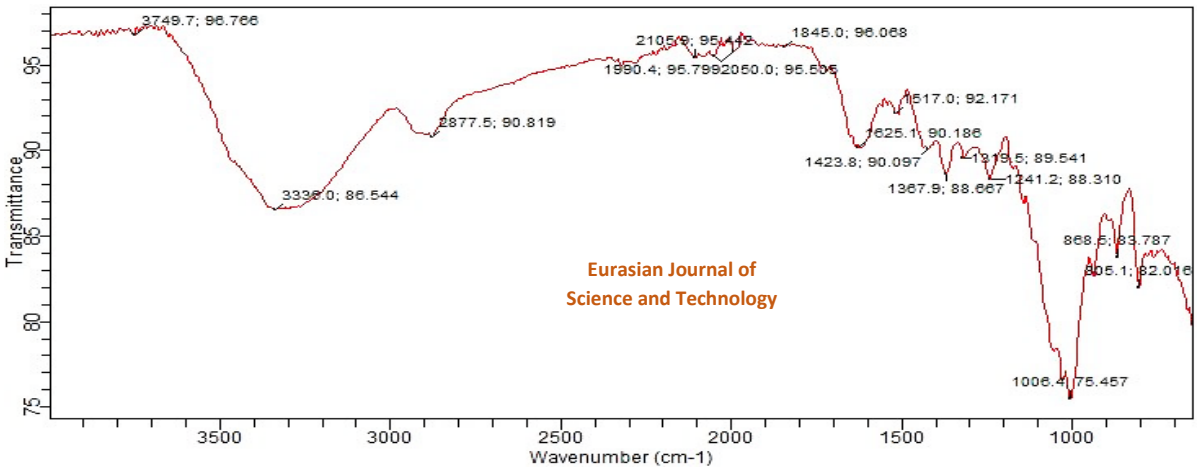

Figure 1. FTIR Spectra of RTR [15]

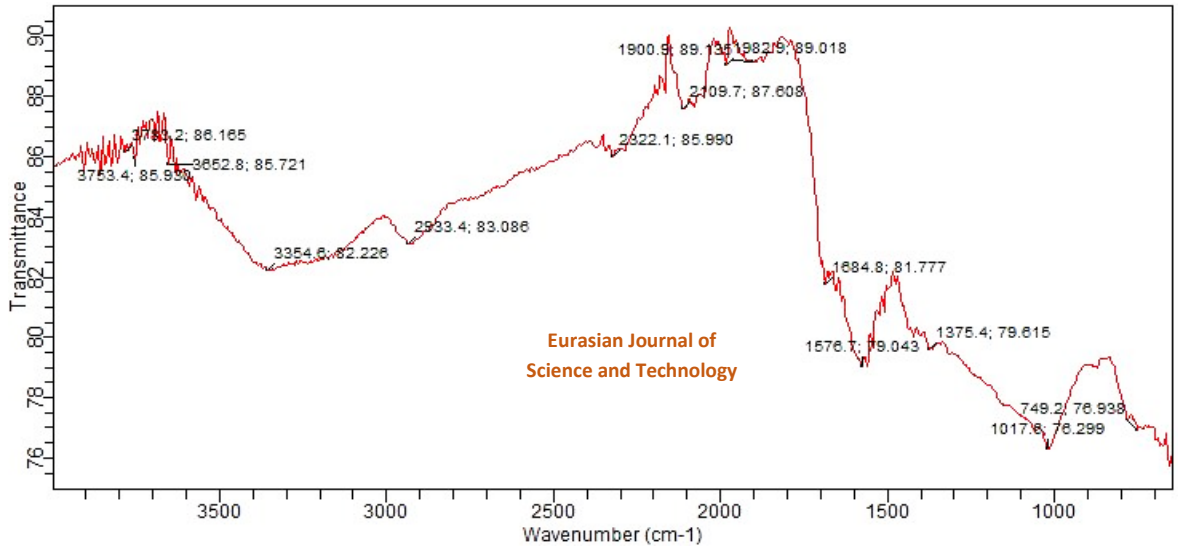

Figure 2 FTIR Spectra of RTB [15]

SEM Analysis

The surface morphologies of RTR and RTB were studied. Figures 3 and 4 represent the SEM micrographs of the RTR and RTB, respectively, at 500X magnifications. Figures 4 (SEM image of RTB) demonstrates a rough and aggregated surface morphology with better and clearer surface porosity, as compared with Figure 3. Activated carbons are known to be good adsorbents in water treatment because of their high porosity [11]. The nature of SEM image of RTB could be attributed to the pyrolysis prior to chemical activation of the sample. The data from semi-quantitative elemental analysis using EDX attached to SEM are illustrated in Figures 5 and 6 representing EDX of RTR and RTB, respectively. The results revealed the C to O ratio in the untreated powdered seed and activated carbon to be 1.29 and 2.50,

respectively. Materials with high carbon content and less oxygen content are known to be useful as adsorbents for the adsorption process [23].

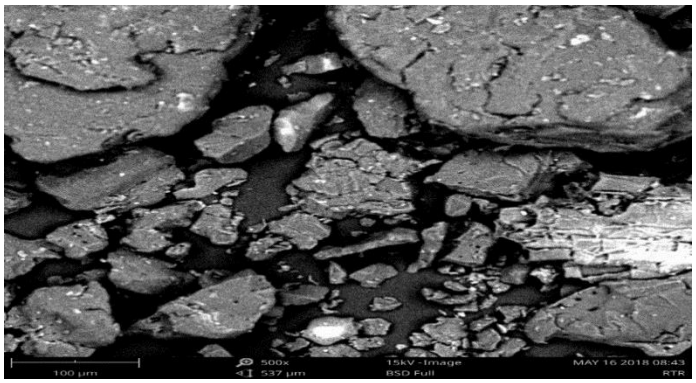

Figure 3 SE image of RTR at 500x Mag [15]

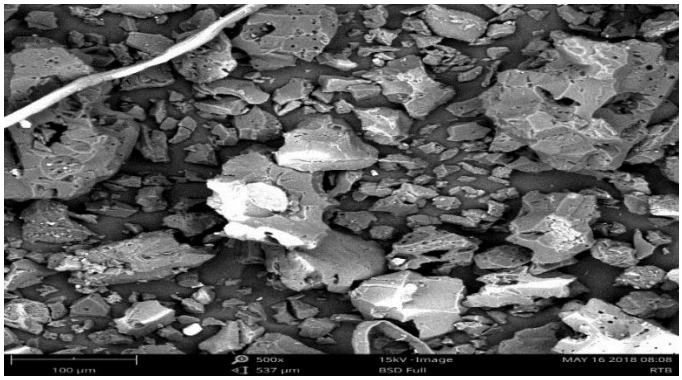

Figure 4 SE image of RTB at 500x Mag [15]

Element	RTR	
	Weight Percentage (%)	Atomic Percentage (%)
Carbon(C)	56.37	63.25
Oxygen(O)	43.63	36.75
C/O ratio	1.2920	

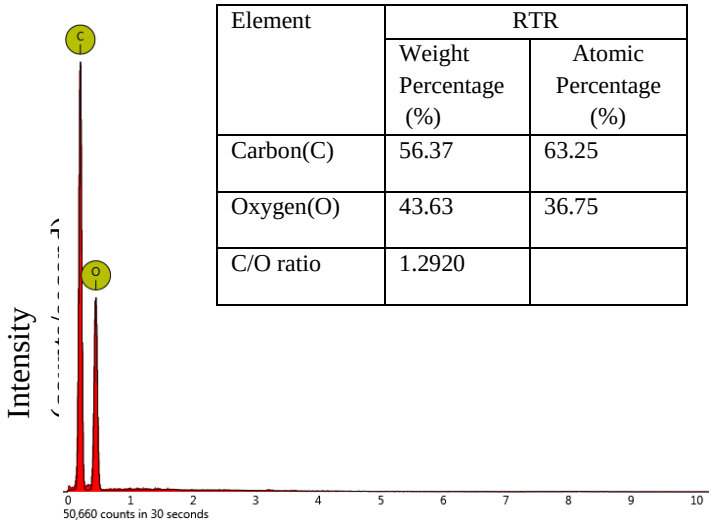

Figure 5 EDX spectrum of RTR

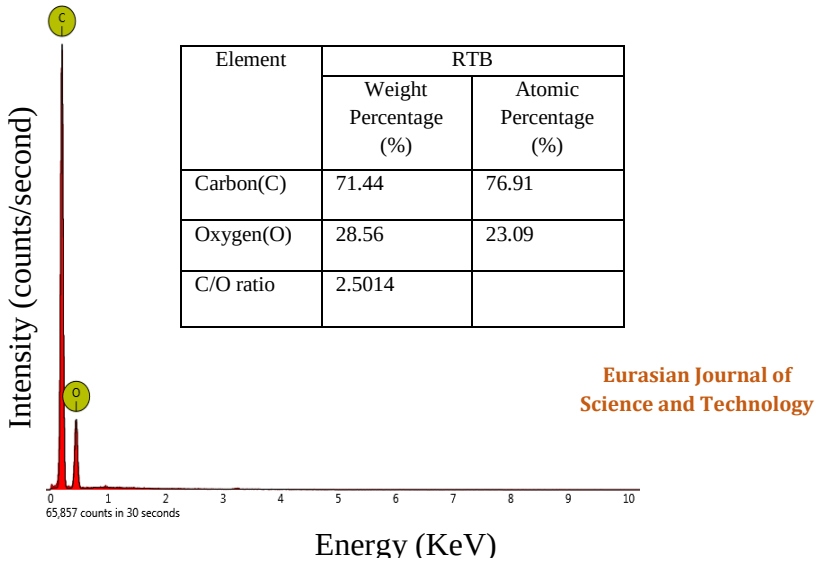

Element	RTB	
	Weight Percentage (%)	Atomic Percentage (%)
Carbon(C)	71.44	76.91
Oxygen(O)	28.56	23.09
C/O ratio	2.5014	

Figure 6 EDX spectrum of RTB

Effect of Adsorption Conditions

Contact Time Effect

The influence of contact time was experimented on the MB dye adsorption onto RTR and RTB to determine the adsorbent-adsorbate equilibrium time. The evaluation was done by shaking 0.1 g of the adsorbent with 50 mL of stock MB dye solution at room temperature for a contact time of 10, 20, 30, 40, 50, 60, 90, and 120 min. Figure 7 depicts the plot of percentage uptake of MB dye against the contact time. The plot showed an increase in the percentage uptake with increasing time for both materials with the activated carbon showing a better performance. Rapid sorption of MB dye was observed at the initial stage, which could be due to the availability of abundance of unoccupied sites on the adsorbent surfaces [24]. The percentage uptake became steady after 30 min for both adsorbents, which can be attributed to the adsorbents' surfaces being almost occupied by MB dye molecules. The responses of the adsorbents to time in the present work were similar to previous reports by AbdulRahman *et al.* [25].

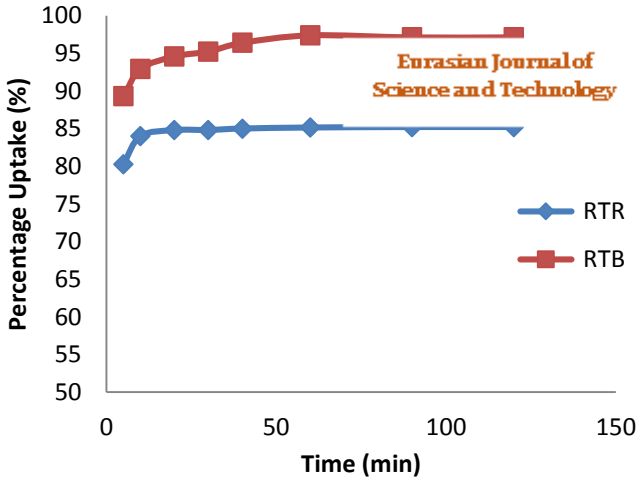

Figure 7. Percentage uptake of MB dye against time

Initial pH Effect

The pH of a solution plays a vital role in the adsorption of pollutants from aqueous solution. The solution pH enhances the surface charge of an adsorbent and predicts the degree of the ionisation and speciation of the material adsorbate. The pH effect experiment was carried with solution pH of 1, 3, 5, 7, and 9 for 30 minutes. The pH was controlled using 0.1 M HCl or 0.1 M NaOH. The plots of percentage uptake of MB dye against pH are presented in Figure 8. The highest percentage of the dye uptake was observed to 84.213 and 96.999% for RTR and RTB, respectively, at the initial solution pH of 5. A comparable result was reported by Olasehinde and Abegunde [5]. Low performances of the adsorbents at low pH may be may be caused by the presence of very active H^+ that are competing with cations on the dye molecule for the adsorption sites. However, the activated carbon showed a better response to the change in solution pH. The superiority showed by RTB could be due to the pre-surface treatment done on the adsorbent prior to the adsorption process. The behaviour of both adsorbents to different solution pH was similar to what was obtained by Hameed *et al.* [26].

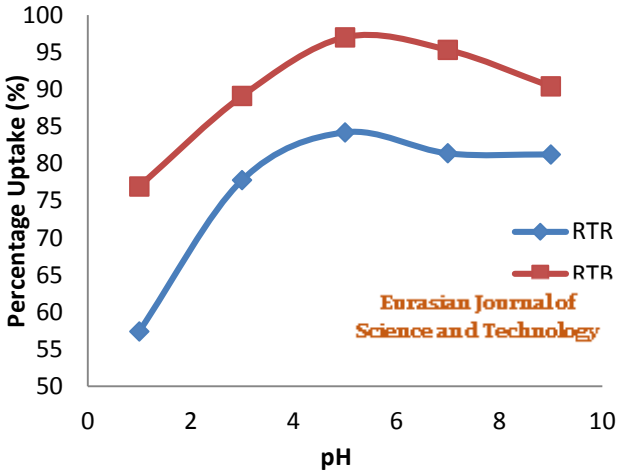

Figure 8 Percentage uptake of MB dye against pH

Temperature Effect

The temperature dependence of the adsorption of MB dye molecule onto RTR and RTB was investigated at the temperature range of 298, 303, 308, 313, and 318 K. The curves of percentage uptake versus temperature are plotted in Figure 9. The maximum adsorption of 82.789 and 93.911% were attained for RTR and RTB, respectively, at 298 K. This showed that the adsorption was favoured at room temperature, indicating an increase in the system temperature will amount to desorption of the adsorbed dye molecules. The response to the change in temperature may be due to the mobility resistivity of the MB dye molecule in the aqueous system by higher thermal energy.

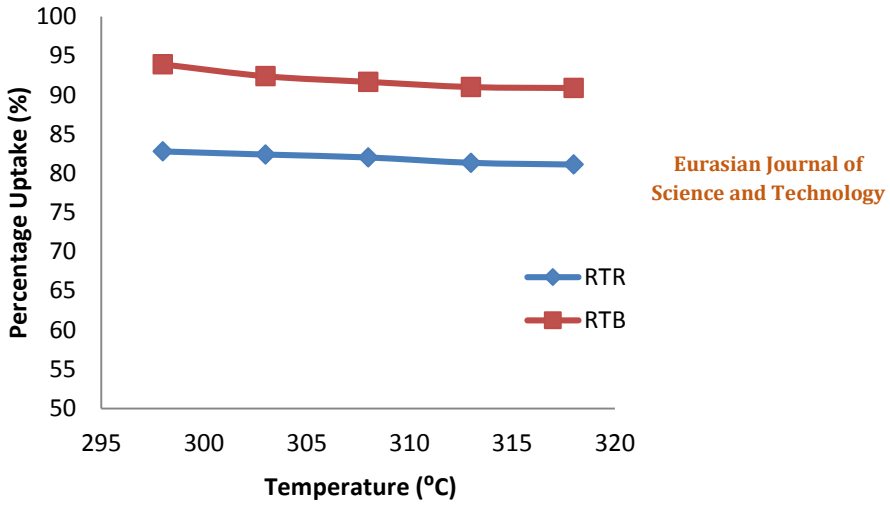

Figure 9 Percentage uptake of MB dye against temperature

Initial Concentration Effect

The concentration effect on the adsorption of MB dye onto RTR and RTB were investigated with 20, 40, 60, 80, and 100 mg/l as initial MB dye concentrations. The plot of the percentage MB dye uptake against the initial dye concentration is presented in Figure 10. The plot revealed a decrease in MB dye removal with the increasing MB dye concentration. The maximum adsorption of 96.017% at 10 mg/L decreased gradually to 83.947% at 100 mg/L for raw *Raphia taedigera* seed powder, and 99.671% at 10 mg/L to 94.127% at 100 mg/L for the activated carbon. The increase in the solution concentration means an increase in the number of active species in the solution. Therefore, the reduction observed in the performances of the adsorbents may be due to the absence of active binding sites to accommodate more MB dye ions at the surfaces of the fixed quantity of adsorbents [27]. The attributes can be comparable with earlier reports by Vaizogullar *et al.* [28] and Wang *et al.* [29] that adsorption process is concentration-dependent.

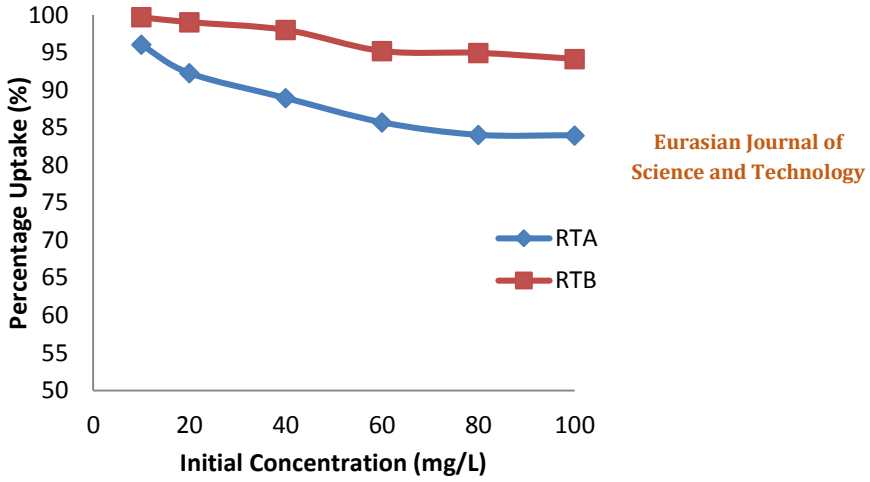

Figure 10 Percentage uptake of MB dye against initial MB concentration

Adsorbent Dosage Effect

Adsorbent supplies the needed binding sites for the pollutants uptake. Therefore, its quantity

largely influences the adsorption. The influence of adsorbent dosage in the sorption of MB dye onto RTR and RTB was determined with adsorbent doses of 0.1, 0.2, 0.3, 0.4, 0.5, and 0.6 g. Figure 11 shows the plots of the percentage uptake against the adsorbent dose in Figure 14. According to Figure 11, the percentage uptake of the MB dye molecule increased with increasing adsorbent dose. The percentage increased steadily from 95.089% by 0.1 g to 99.989% by 0.6 g of RTB, and 84.922% by 0.1 g to 90.893% by 0.6 g of RTR. The improvement in the percentage dye uptake at a higher mass of the adsorbents may be as a result of the higher number of active binding sites due to increased in the bulk of the adsorbents [26,16]. Similar observation was made by Sari *et al.* [30].

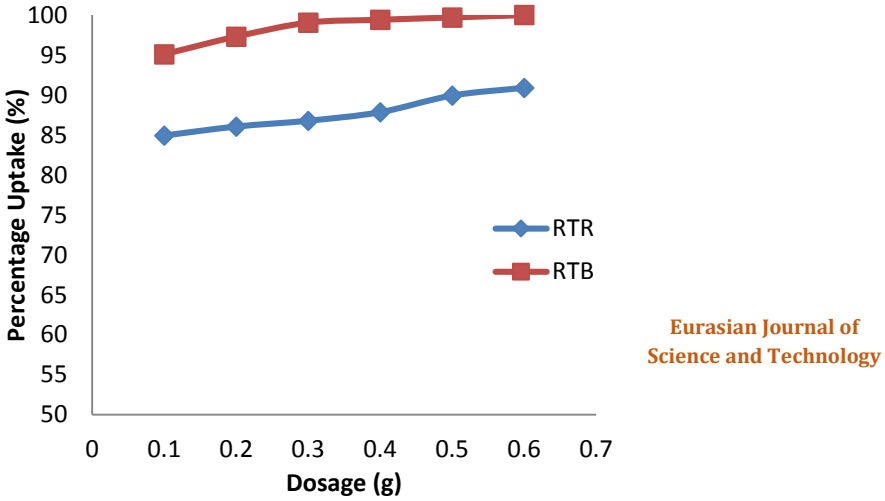

Figure 11 Percentage uptake of MB dye against adsorbent dose

Adsorption Isotherms

The adsorption isotherms explain the adsorbent-pollutant interaction [30]. Hence, it is crucial to establish the best correlation for the equilibrium curves to optimise the use of adsorbents. The isotherm models engaged for this work are Freundlich and Langmuir adsorption isotherm models.

Langmuir Isotherm

Langmuir isotherm presumes the uptake of pollutants by homogeneous surface is monolayer without interaction between adsorbed molecules [29]. Figure 12 demonstrates the curves of C_e/q_e //C_e for the adsorption of the dye molecules onto RTR and RTB at te 298, 308, and 318 K temperature. From the plots, the MB dye adsorption onto the adsorbents are linear with correlation coefficients (R^2) values of between 0.9248-0.9999 across the temperature range indicating favourable adsorption processes between the adsorbents and MB dye. The q_{max} values from the slopes of of C_e/q_e//C_e plotsare presented in Table 1. Based on Table 1, the experimental value of q_{max} was close to the corresponding calculated value of q_e, indicating that the Langmuir isotherm can be a good fit for the adsorption of MB dye onto RTR and RTB. Furthermore, the value of a dimensionless constant (R_L) was calculated and presented in Table 1. The R_L value at each temperature is greater than zero but less than 1 (i.e., 1 >R_L > 0), is an indication of a favourable adsorption process.

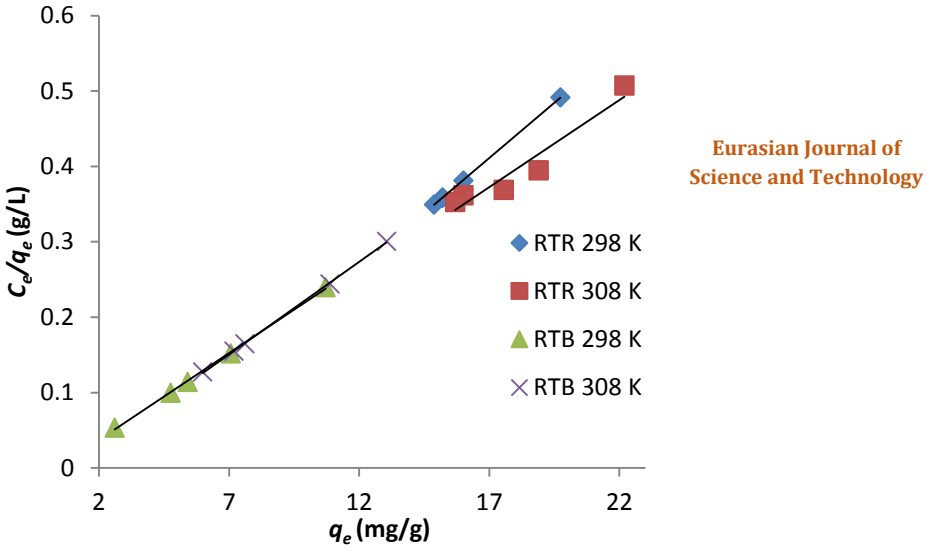

Figure 12 Langmuir isotherm plots of adsorption of MB dye by RTR and RTB

Freundlich Isotherm

The model assumes that adsorption occurs on a heterogeneous surface with an uneven distribution of sorption heat through a multilayer adsorption mechanism [31]. Freundlich isothermplots of log q_e vs. log C_e for the MB dye molecule adsorption by RTR and RTB are exhibited on Figure 13. The k_F and n values for the intercepts and slopes, respectively, are presented in Table 1. The Freundlich isotherm also exhibited high correlation coefficients ranging from 0.9369 to 0.9991 across the working temperature for both adsorbents. The *1/n* values are less than 1 at all temperature indicating a normal Langmuir isotherm. Deducing from the correlation coefficient, (R^2), and slope (*1/n*), it can be mentioned that Langmuir isotherm model can best represent the adsorption data.

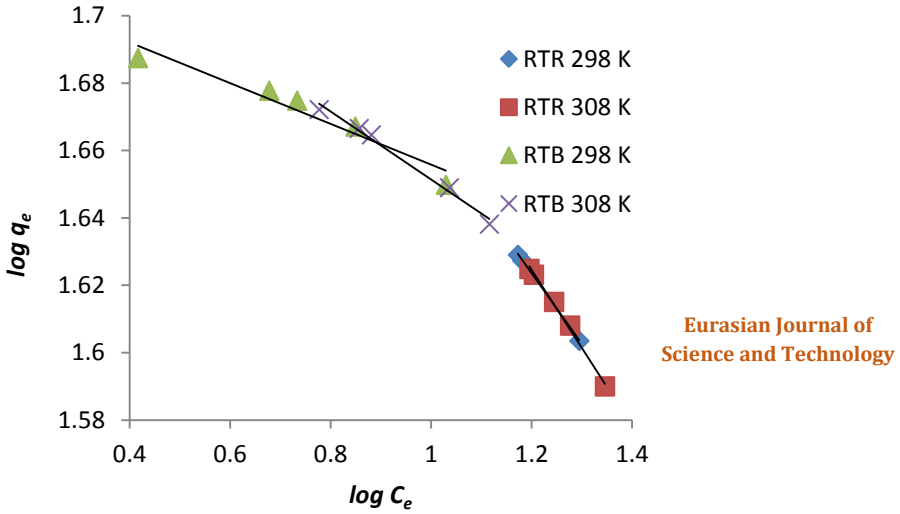

Figure 13 Freundlich isotherm plots of MB dye adsorption by RTR and RTB

Table 1 Adsorption isotherm parameters

Isotherms Equation	Parameters	RTR		RTB	
		298 K	308 K	298 K	308 K
Langmuir $\frac{Ce}{qe} = \frac{1}{KLqm} + \frac{Ce}{qm}$	Exp. q_m (mg/g)	34.130	43.290	43.290	40.816
	Cal. q_e (mg/g)	40.136	38.904	44.649	43.470
	K_L (L/mg)	0.334	1.138	2.567	1.184
	R_L	0.029	0.009	0.004	0.008
	R^2	0.9999	0.9248	0.9992	0.9996
Freundlich $log\ qe = log\ Kf + \frac{1}{n} log\ Ce$	$1/n$	0.210	0.231	0.060	0.101
	N	4.771	4.333	16.556	9.921
	K_f	75.007	79.708	52.024	56.520
	R^2	0.9991	0.9960	0.9369	0.9888

Adsorption Kinetics

The MB dye/RTR and MB dye/RTB mechanism of adsorption and the potential rate-determining steps are investigated engaging pseudo-first-order and the pseudo-second-order kinetic models. Figure 14 is a plot of $log(q_{eq} - q_t)$ against t for the pseudo-first-order kinetic model. From the plots, the pseudo-first-order parameters values (q_e, R, *and* k_1)were obtained and computed in Table 2. The $q_{e(cal)}$ valueswere close to their corresponding q_{exp} values. However, the R^2 values range from 0.4188 to 0.7144 for the adsorbents, indicating a relatively weak relationship between the adsorption data. Base on the R^2 values, the pseudo-first-order kinetic model cannot be mentioned to be appropriate to represent the experimental data for the concentration understudy at these temperatures [9,42]. The pseudo-second-order kinetic model plots were presented in Figure 15 as plots of t/qt against t.

The pseudo-second-order parameters (q_e, k_2, and $R)^2$ were calculated for the RTR and RTB, as presented in Table 2. According to Table 2, the values of R^2 were obtained to be between 0.9999 to 1 for both RTR and RTB at all temperatures. The high values of R^2 indicated a strong inter-dependence nature of the adsorption data. The calculated values of q_e were also seen to be closed to the corresponding experimental q_e values for the adsorption of MB dye onto both RTR and RTB. This result indicated showed the adsorption of MB dye by RTR and RTB followed pseudo-second-order kinetic model for the concentration of the dye at all temperatures. The relevance of the pseudo-second-order model at constant concentration suggests that chemical reaction might be a contributing factor for adsorption of MB dye onto the RTA and RTB. The result of similar findings was reported by Chiou *et al.* [32] and Ofomaja and Ho [33].

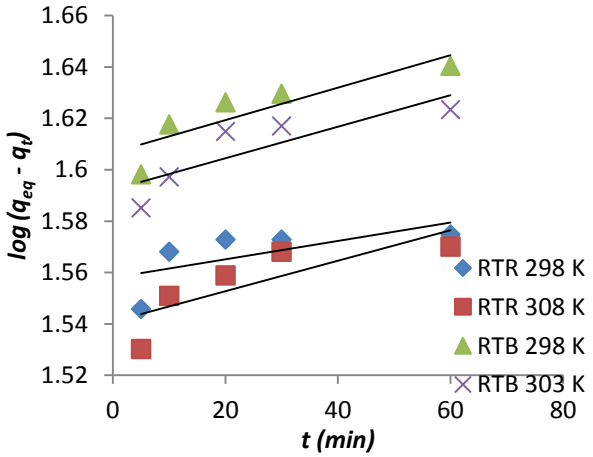

Eurasian Journal of Science and Technology

Figure 14 Pseudo-first-order kinetic plots of MB dye adsorption by RTR and RTB

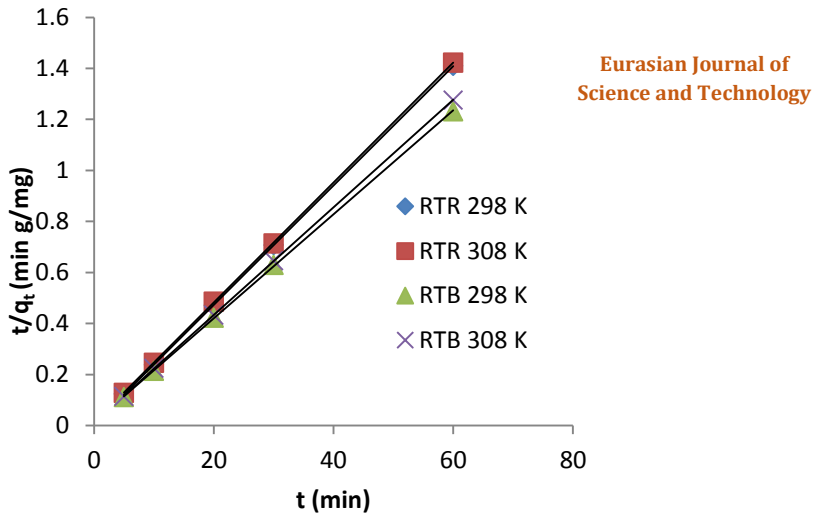

Figure 15 Pseudo-second-order kinetic plots of MB dye adsorption by RTR and RTB

Table 2 Results of adsorption isotherm parameters

Kinetic model	Parameter	RTR		RTB	
		298 K	308 K	298 K	308 K
Pseudo-first-order $\frac{1}{qt}=\frac{K1}{qet}+\frac{1}{qe}$	$q_e(mg/g)$	36.133	34.690	40.420	39.102
	K_1	0.0009	0.0014	0.0014	0.0014
	R^2	0.4188	0.6445	0.7610	0.7144
Pseudo- second-order $\frac{t}{qt}=\frac{1}{K2q2e}+\frac{1}{qe}t$	$q_e(mg/g)$	42.735	42.553	49.020	47.393
	$K_2(g/mg/min)$	338200	156101	186670	190350
	R^2	1.0000	1.0000	0.9999	1.0000

Thermodynamic studies

Thermodynamic constants are the standard factors for the practical use of an adsorption technique. Parameters like enthalpy change (ΔH), entropy change (ΔS), and Gibbs free energy change (ΔG) were evaluated for deep understanding of the temperature dependence of the adsorption processes [5]. The plots of *lnKc* against *1/T* for MB dye adsorption by RTR and RTB are presented in Figure 16. The ΔH^0 *and* ΔS^0 values obtained from the plots are tabulated in Table 3. From Table 3, negative values of ΔG^0 indicate feasible and spontaneous nature of the adsorbents for the removal of MB dye molecule from aqueous solution. The values were within -20 – 0 KJ/mol revealed that the adsorption processes are physisorption. The ΔG^0 value increased with an increase in temperature, indicating favoured adsorption at low temperature. The negative values obtained for ΔH^0 for the MB adsorption dye onto RTR and RTB indicated that the adsorption processes are exothermic. Negative values of ΔS^0 for RTR and RTB showed a decrease in the disorderliness degree for the adsorption of MB dye molecules. This showed that the dye molecules were orderly adsorbed onto the surface of the adsorbents. The result of the present study was in agreement with the report of Olasehinde *et al.* [31].

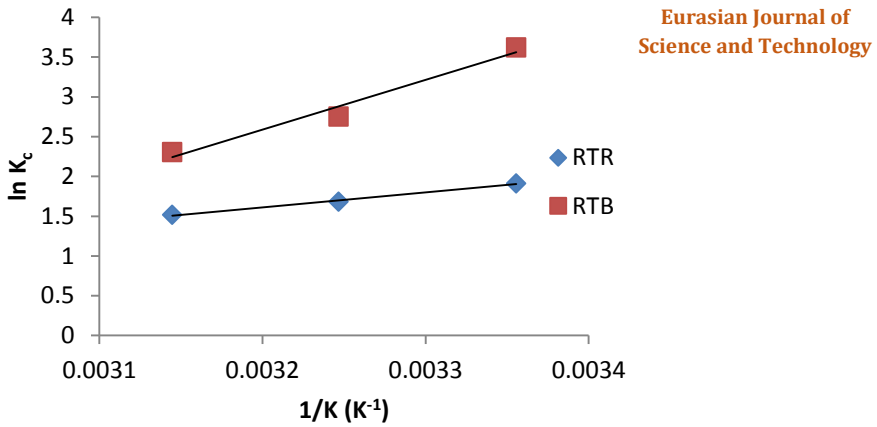

Figure 16 Plots of lnK_c against $1/K$ of MB dye adsorption by RTR and RTB

Table 3 Thermodynamic parameters

Adsorbent	Temperature	ΔG⁰ (KJ/mol)	ΔH⁰ (KJ/mol)	ΔS⁰ (J/K)
	298 K	-4.7175		
RTR	308 K	-4.3514	-15.6270	-36.6090
	318 K	-3.9853		
	298 K	-8.8209		
RTB	308 K	-7.3755	-51.8935	-144.5389
	318 K	-5.9301		

Conclusion

Activated carbon was prepared successfully from *Raphia taedigera* seed and activated with NaOH solution. The activated carbon (RTB) and the raw powder seed were characterised and used for methylene blue dye removal from aqueous solution. FTIR analysis revealed the presence of functional groups such as hydroxyl, carboxylic, ester, aldehydes, and kenotic groups that are known to aid adsorption process. SEM-EDX revealed the surface morphologies of the materials as rough and aggregated surface with pores at the surfaces. The highest percentage of MB dye uptake by RTR is 85.19% at 90 min, 84.21% at pH 5, 82.79% at 298 °C, 96.02% at 10 mg/L, and 90.89% at 0.6 g for the evaluation of time, pH, temperature, initial dye concentration, and the adsorbent dosage, respectively, while the highest percentage of MB dye uptake by RTB is 97.39% at 60 min, 97.00% at pH 5, 93.91% at 298 °C, 99.67% at 10 mg/L, and 99.91% at 0.6 g for the evaluation of time, pH, temperature, initial MB dye concentration, and adsorbent dosage, respectively. The adsorption modelling results revealed the adsorption data fit most to Langmuir isotherm and pseudo-second-order kinetic models predicting a monolayer nature of the MB dye on the surfaces of both adsorbent materials. The thermodynamic studies for the adsorption of MB dye onto RTR and RTB revealed exothermic, feasible, spontaneous, and physisorption nature of the adsorption onto the two adsorbents within the temperature range for this study. The results of this study showed that the activated carbon displayed a better performance under all experimental conditions. The advantage of AC over the untreated seed powder can be attributed to the pyrolysis and alkali chemical activation done on the RTB. Finally, it can be concluded that the two materials are excellent sorbents to remove

methylene blue dye molecules from aqueous solution.

Conflict of interest

The authors declare no conflicts of interest about this work.

References

[1] Ö. Dülger, F. Turak, K. Turhan, M. Özgür, *Int. sch. Res.,* **2013,** 2013, 1–9. [Crossref], [Google Scholar], [Publisher]

[2]C. I, Pearce, J. R. Lloyd, J. T. Guthrie, *Dyes Pigm.,***2003**, 58, 179–196. [Crossref], [Google Scholar], [Publisher]

[3]G. Crini, *Bioresour. Technol.,***2006**, 97, 1061-1085. [Crossref], [Google Scholar], [Publisher]

[4]S. Hajati, M. Ghaedi, F. Karimi, B. Barazesh, R, Sahraei, A. Daneshfar, *J. Ind. Eng. Chem.,***2014**, 20, 564–571. [Crossref], [Google Scholar], [Publisher]

[5]E. F. Olaseinde, S. M. Abegunde., *Adv. J. Chem. A*, **2020,** 3, 663–679.[Crossref], [Google Scholar], [Publisher]

[6]R. Gong , Y. Sun, J. Chen, H. Liu, C. Yang, *Dyes Pigm.,***2005**, 67, 175 - 181. [Crossref], [Google Scholar], [Publisher]

[7]R. Saravanan, E. Sacari, F. Gracia, M. M. Khan, E. Mosquera, V. K. Gupta, *Mol. Liq. J.,***2016**., 221: 1029 – 1033. [Crossref], [Google Scholar], [Publisher]

[8]T. A. Saleh, V. K. Gupta, *J. Colloid Interface Sci.,***2012**; 371: 101–106. [Crossref], [Google Scholar], [Publisher]

[9]G. E. J. Poinern, S. Brundavanam, D. Fawcett, *Biomed. Eng.,***2012** 2, 218-240. [Crossref], [Google Scholar], [Publisher]

[10] N. A. Abdulrahman, A. Rotibi, S. M. Abegunde, *Int. j. sci. Res.,* **2020**, *10, 164 - 174.* [Crossref], [Google Scholar], [Publisher]

[11] S.M. Abegunde, K.S. Idowu, A.O. Sulaimon, *J. Chem. Rev.,***2020** 2, 103-113. [Crossref], [Google Scholar], [Publisher]

[12] N. V. Chagas, J. S. Meira, F. J. Anaissi, F. L. Melquiades, S. P. Quinaia, M. L. Felsner. K. C. Justi, *Rev. Virtual Quim*, **2014**. 6 , 1607 - 1623. Revista Virtual de Quimica, 6(6), 1607-1623. [Crossref], [Google Scholar], [Publisher]

[13] E. Rostami, R. Norouzbeigi, A. R. Kelishami, *Adv. Environ. Technol.*, **2018**, 1- 12. [Crossref], [Google Scholar], [Publisher]

[14] M. Lesaoana, R. P. V. Mlaba, F. M. Mtunzi, M. J. Klink, P. Ejidike, V. E. Pakade , *S. Afr. J. Chem. Eng*., **2019**, 28, 8–18. [Crossref], [Google Scholar], [Publisher]

[15] E. F. Olasehinde, S. M. Abegunde, *Res. Eng. Struct. Mater.*, **2020**, 6, 167-182. [Crossref]

[16] S. M. Abegunde, *Asian J.Chem.Sci.,***2018**, 5, 1-8. [Crossref], [Google Scholar], [Publisher]

[17] I.O. Awonyemi, M.S. Abegunde, T.E. Olabiran, *Eurasian.Chem.Commun.*, **2020**, 2, 938 - 944. [Crossref], [Google Scholar], [Publisher]

[18] A. Rotibi, K. Adesina, S. M. Abegunde, *WJAETS,***2022**,6,040–046. [Crossref], [Google Scholar]

[19] A. Mittal, J. Mitta, A, Malviya, D, Kaur , V. K. Gupta, *J. Colloid Interface Sci.,* **2010,** 342, 518 – 527. [Publisher]

[20] S. Kundu, V. K. Gupta, *J. Chem.Eng.* **2006**, 122, 93–106.

[21] E. F. Olasehinde, A. V. Adegunloye, M. A. Adebayo, A. A. Oshodi, *Anal.Lett.,***2018**, 51, 2710-2732. [Crossref]

[22] M. Kilic, E. Apaydin-Varol, A. E. Pu¨tu¨n, *J.Hazard.Mater.*, **2011**, 189, 397–403. [Crossref], [Google Scholar], [Publisher]

[23] C. Xiong, Q. Jia, X. Chen, G. Wang, C. Yao, *Ind.Eng.Chem.Res.,***2013**, 52, 4978–4986. [Crossref], [Google Scholar], [Publisher]

[24] Y. D. Lamidi, S. S. Owoeye, S. M. Abegunde, *Glob. J. Eng. Technol. Adv*., **2021,** 6, 076–090. [Crossref], [Google Scholar], [Publisher]

[25] A. AbdulRahman, A. A. Latiff, Z. Daud, M. B. Ridzuan, A. H. Jagaba, *Mater. Sci. Eng.***2016**, 136, 1-6.10.[Crossref], [Google Scholar], [Publisher]

[26] B. H. Hameed, A. T. M. Din, A. L. Ahmad, *J. Hazard.Mater.,***2007**, 141, 819–825. [Crossref], [Google Scholar], [Publisher]

[27] S. M. Abegunde, K. S. Idowu, O. M. Adejuwon, T. Adeyemi-Adejolu, *Resources, Environment and Sustainability,* **2020,** 1, 1 – 9.[Crossref], [Google Scholar], [Publisher]

[28] A. I. Vaizogullar, A. Balci, I. Kula, M. Ugurlu, *Turk.J.Chem.***2016**, 40, 565–575. [Crossref], [Google Scholar], [Publisher]

[29] D. Wang, H. Shan, X. Sun, H. Zhang, Y. Wu, *Adsorp Sci Technol.,* **2018,** 36, 1366 – 1385. [Crossref], [Google Scholar], [Publisher]

[30] A. Sari, M. Tuzen, D. Citak, M. Soylak, *J. Hazard.Mater.,***2007**, 149, 283–91. [Crossref], [Google Scholar], [Publisher]
[31] E. F. Olasehinde, S. M. Abegunde, M. A. Adebayo, *Casp.J.Environ.Sci.,***2020,** 18, 329–344. [Crossref]
[32] M. S. Chiou, P. Y. Ho, H. Y. Li, *Dyes Pigm.,***2004**, 60, 69 - 84. [Crossref], [Google Scholar], [Publisher]
[33] A. E. Ofomaja, Y. Ho, *J. Hazard.Mater.,***2007**, 139, 356–362. [Crossref], [Google Scholar], [Publisher]